

## PAPER

[View Article Online](#)  
[View Journal](#) | [View Issue](#)Cite this: *Dalton Trans.*, 2024, **53**, 9433

## Coordination of azol(in)ium dithiocarboxylate ligands to Au(III): unexpected formation of a novel family of cyclometallated Au(III) complexes, DFT calculations and catalytic studies†

Paula Pérez-Ramos, María A. Mateo, David Elorriaga,<sup>id</sup> \* Daniel García-Vivó,<sup>id</sup> Raquel G. Soengas<sup>id</sup> \* and Humberto Rodríguez-Solla<sup>id</sup> \*

A series of cyclometallated gold(III) complexes **21–27** of general formula [Au(dppta)(azdtc)Cl] (dppta = *N,N*-diisopropyl-*P,P*-diphenylphosphinothioic amide- $\kappa^2$ C,S; azdtc = azol(in)ium-2-dithiocarboxylate- $\kappa^1$ S) were prepared and characterized by spectroscopic and diffractometric techniques. Treatment of [Au(dppta)(azdtc)Cl] complexes with methanol led to their quantitative transformation into a novel family of (C $\wedge$ S, S $\wedge$ S)-cyclometallated gold(III) complexes of general formula [Au(dppta)(azmdt)] (azmdt = azol(in)ium-2-(methoxy)methanedithiol- $\kappa^2$ S,S) **28–34**. All the [Au(dppta)(azdtc)Cl] complexes **21–27** catalyzed the alkylation of indoles, whereas [Au(dppta)(azmdt)] complexes **28–34** were inactive. Among the synthesized derivatives, complex **22** displayed the highest catalytic activity, leading to a series of functionalized indoles in excellent yields.

Received 22nd April 2024,  
Accepted 13th May 2024

DOI: 10.1039/d4dt01184h

rsc.li/dalton

## Introduction

Gold chemistry has attracted considerable attention in the past few years due to the potential applications in medicine, optoelectronics and catalysis.<sup>1</sup> These studies have mostly focused on Au(I) complexes, with considerably less attention being paid to Au(III) complexes. However, recent studies have put Au(III) complexes on the spotlight as hot topic of research because of their potential interest as antitumor and antibacterial agents,<sup>2</sup> their application in the development of luminescent materials<sup>3</sup> and their ability to activate unsaturated groups in diverse catalytic processes.<sup>4,5</sup> One of the major disadvantages of Au(III) complexes is their inherent instability, due to their tendency to undergo reduction.<sup>6</sup> To avoid reduction, an interesting approach is the stabilization of the Au(III) centre by coordination to a cyclometallated ligand to render complexes of the general formula [AuX<sub>2</sub>(C–Y)], where C–Y represents a bis-coordinated ligand with a Au–C  $\sigma$ -bond and a coordinate bond through N, P or S donor atom (Fig. 1).<sup>7</sup>

These Au(III) complexes have a square planar geometry with four coordination sites around the metal centre and through rational ligand design, the reactivity of the complexes can be modulated “à la carte”. For instance, the properties of Au(III) complexes can be tuned to achieve a right balance between stability and reactivity and obtain perfect candidates for their use as catalysts in various organic transformations.

In that sense, N-heterocyclic carbene (NHC) ligands are well known in gold chemistry due to their easy tuneability, electron-rich nature and steric bulk.<sup>2a,8</sup> Related to NHC ligands, zwitterionic dithiocarboxylate azol(in)iums can coordinate to metals as monodentate, chelate bidentate or bridging bidentate (Fig. 2).<sup>9</sup> Even though the potential of these ligands has been studied with a certain number of transition metals,<sup>10</sup> the

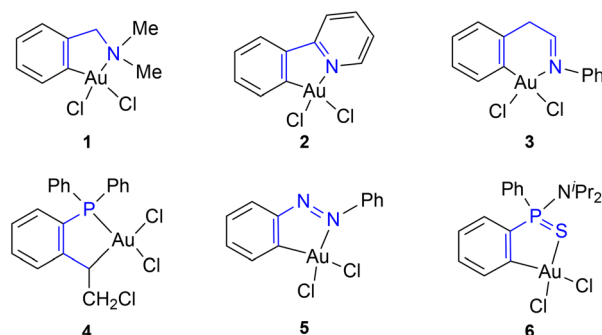


Fig. 1 Some relevant cyclometallated gold(III) complexes.

Departamento de Química Orgánica e Inorgánica and Instituto Universitario de Química Organometálica “Enrique Moles”, Universidad de Oviedo, Julián Clavería 8, 33006 Oviedo, Spain. E-mail: hrsolla@uniovi.es, rsoengas@uniovi.es, elorriaga@uniovi.es

† Electronic supplementary information (ESI) available. CCDC 2346965–2346967. For ESI and crystallographic data in CIF or other electronic format see DOI:

<https://doi.org/10.1039/d4dt01184h>

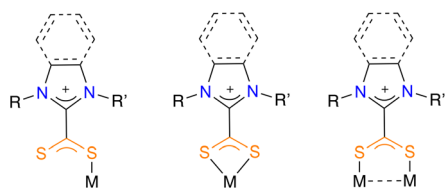


Fig. 2 Bonding modes of azol(in)ium-2-dithiocarboxylate ligand to metal centres.

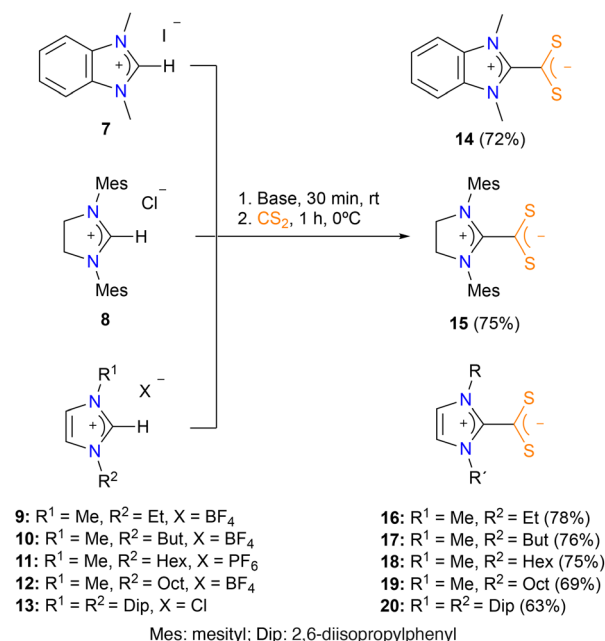
presence of coordination complexes of dithiocarboxylate azolium ligands and gold in the literature is very limited. The first report dates back to 1987, when Borer *et al.* described the formation of Au(I) complexes by reaction of dithiocarboxylate azolium ligands and NaAuCl<sub>4</sub>·2H<sub>2</sub>O.<sup>11</sup> Later on, Wilton-Ely and co-workers reported an in-depth study of the coordination of these zwitterionic ligands to Au(I), as well as their suitability for an efficient stabilization of gold nanoparticles.<sup>12</sup> In this same vein, these authors subsequently studied the chemisorption of dithiocarboxylate azolium ligands on solid gold substrates.<sup>13</sup>

Here we report the synthesis of a novel class of cyclometallated Au(III) compounds bearing azol(in)ium-2-dithiocarboxylate  $\kappa^1$ S-donor ligands as auxiliary ligands. Moreover, their unprecedented transformation into  $\kappa^2$ S,S-azol(in)ium-2-(methoxy)methanedithiolate cyclometallated gold(III) complexes was also achieved. Additionally, catalytic performance of all the synthesized complexes was studied for the alkylation of indoles.

## Results and discussion

### Synthesis of the azol(in)ium dithiocarboxylate ligands

The most convenient procedure to synthesize the azol(in)ium dithiocarboxylate zwitterionic ligands is by means of the deprotonation of azolium salts and subsequent addition of CS<sub>2</sub>. Thus, we treated commercially available benzimidazolium 7, imidazolinium 8, and imidazolium 9–13 salts with Cs<sub>2</sub>CO<sub>3</sub> in acetonitrile for 30 minutes and then we added carbon disulfide. After stirring the resulting mixture at r.t. for 4 hours, compounds 14, 15 and 20 were obtained in almost quantitative yields (Scheme 1). However, this protocol was unsuccessful for *N*-alkyl substituted imidazolium salts, which need a stronger base for the deprotonation step. Therefore, treatment of imidazolium salts 9–12 with <sup>t</sup>BuOK in THF for 30 minutes and subsequent addition of carbon disulfide, afforded the corresponding azolium dithiocarboxylate zwitterionic ligands 16–19 as orange-red solids (Scheme 1). Ligands 14, 15 and 20 were previously reported in the literature,<sup>9d,f</sup> whereas ligands 16, 17, 18 and 19 have been prepared and characterized for the first time in this work. The <sup>13</sup>C{<sup>1</sup>H} NMRs of all these ligands show a characteristic signal around 224 ppm which correspond to the carbon atom of the CS<sub>2</sub> core. In general terms, the data obtained for ligands 14–20 fit with their zwitterionic nature and agree with the data previously reported in the literature.<sup>9d,f</sup>



Scheme 1 Synthesis of dithiocarboxylate azol(in)ium zwitterionic ligands 14–20.

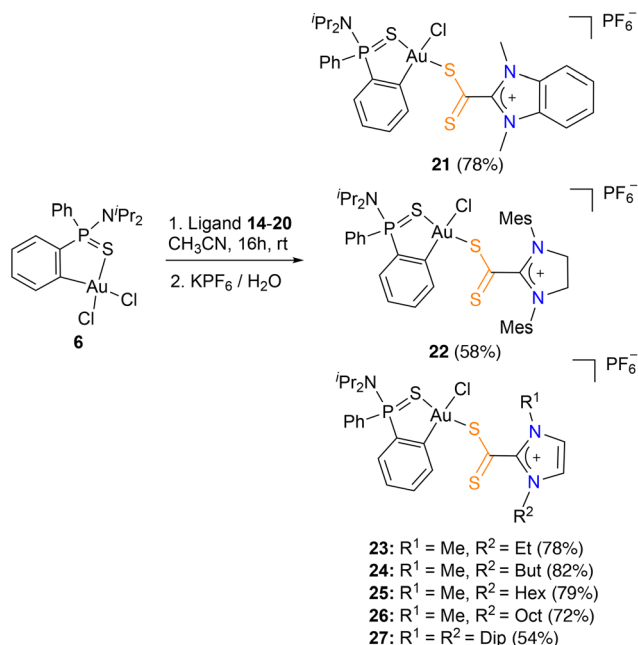
### Formation of azol(in)ium dithiocarboxylate Au(III) complexes

Our recent studies on Au(III) complexes have focused on the synthesis of (S<sup>^</sup>C)-cycloaurated compounds for the evaluation of their chemical and biological properties.<sup>14</sup> Taking into account our previous experience, we decided to investigate the complexation of (S<sup>^</sup>C)-cycloaurated dichloride complex 6<sup>7b</sup> to azol(in)ium dithiocarboxylate ligands.

Thus, reaction of stoichiometric amounts of the azol(in)ium dithiocarboxylate zwitterionic ligands 14–20 with the Au(III) precursor 6 in acetonitrile for 16 hours at room temperature and subsequent addition of aqueous KPF<sub>6</sub> afforded the corresponding azol(in)ium dithiocarboxylate- $\kappa^1$ S complexes 21–27 as red solids in good yields (54–82%) (Scheme 2).

The obtained dithiocarboxylate azol(in)ium complexes 21–27 were fully characterized by multinuclear NMR spectroscopy, MS, IR and, in several cases, X-ray diffraction studies. Two sets of proton and carbon signals were observed, indicating the formation of the two possible isomers, *cis* or *trans*. However, the isomers with the two S atoms in *trans* configuration are preferentially formed in all cases (de 73–94%). This is possibly due to the preferential mutual *trans* disposition of the ligand with the highest *trans* influence (C) and the hardest base (Cl) due to the antisymbiotic effect,<sup>15</sup> a feature commonly observed in gold(III) complexes.<sup>16</sup> The <sup>1</sup>H NMR spectra of complexes 21–27 show that proton *ortho* to the gold ion (7.55–8.16 ppm) is shifted significantly upfield relative to the precursor complex [Au(dppta)Cl<sub>2</sub>] 6 (8.47 ppm). On the other hand, the <sup>13</sup>C{<sup>1</sup>H}-NMR spectra showed a upfield displacement of the signal corresponding to the CS<sub>2</sub> moiety (206.1–210.4 ppm) with respect to the free ligand (224.6–224.7 ppm), which is in accordance with the examples





**Scheme 2** Synthesis of azol(in)ium-2-dithiocarboxylate complexes **21–27**.

of azol(in)ium dithiocarboxylate metal complexes reported so far in the literature (205–225 ppm).<sup>17</sup>

Fortunately, X-ray quality single crystals of the *trans*-isomers of **22** and **27** were obtained from a saturated solution of the compound in THF layered with hexane. The molecular structures of **22** and **27** showing the atomic numbering scheme are depicted in Fig. 3. Diffraction studies revealed a mononuclear compound and confirmed the coordination of the dithiocarboxylate ligand in a  $\kappa^1\text{S}$ -monodentate mode, so that both coordinated sulfur atoms are in a mutual *trans*-disposition. The S1–Au1 and S2–Au1 distances are very similar ( $\sim 2.31$  Å and  $\sim 2.33$  Å, respectively). On the other hand, in contrast with the free ligand, the S3–C19 distance ( $\sim 1.63$  Å) is slightly shorter

than the S2–C19 distance ( $\sim 1.70$  Å) which suggests a greater  $\pi$ -contribution over the S3–C19 bond. However, both bonds are in an intermediate situation between the values expected for single and double C–S bonds (approx. 1.61 Å for the S=C bonds and approx. 1.75 Å for the S–C bonds).<sup>18</sup> The metallacycle in complex **22** differ slightly from the planar geometry, with the phosphorus atom puckered out the plane and the plane S1–P1–C2 tilted  $29.27^\circ$  from the plane formed between S1–Au1–C1. This effect is even more evident in complex **27**, for which this angle is even larger ( $46.6^\circ$ ), which seems to be due to the presence of an S– $\pi$  interaction between S3 and the centroid of the aromatic ring facing it at a distance of 3.51 Å (Fig. 3c); this distance falls within the range described in the literature for this type of S– $\pi$  interactions.<sup>19</sup> All these effects translate into a geometry around the gold atom that deviates slightly from the ideal square planar geometry, as indicated by the structural parameter  $\tau_4$ , with values of 0.06 and 0.09 for **22** and **27**, respectively.<sup>20</sup>

Surprisingly, the outcome of the reaction of the azol(in)ium dithiocarboxylate ligands **14–20** with the gold precursor **6** is strongly dependent on the solvent used. Thus, when the reaction is carried out using methanol as solvent, a new family of cyclometallated complexes **28–34** was obtained (Scheme 3). In these new complexes, a methoxy group bonds to the dithiocarboxyl carbon atom, forming a azol(in)ium-2-(methoxy)methanedithiolate which bonds to the Au(III) metal center in a  $\kappa^2\text{S,S'}$  coordination mode. The new complexes **28–34** were obtained as yellow solids in good yields and characterized by multinuclear NMR. Two chiral centers are present in the product of this reaction; thus, there are two pairs of enantiomers possible from this reaction. The  $^1\text{H}$ -NMR spectra of all complexes showed two identical sets of signals in a 1:1 ratio which correspond with the mixture of *syn/anti*-isomers with respect to mutual orientation of the nitrogen atom of the  $\text{N}^i\text{Pr}_2$  and the oxygen atom of the methoxide motif. The presence of two singlets around 3–3.5 ppm (one for each isomer) confirm the incorporation of the methoxy group. The  $^{31}\text{P}\{^1\text{H}\}$ -NMR spectrum are also consistent with the formation of diastereomeric complexes, showing two distinct signals at 70–80 ppm and a septuplet at around  $-140$  ppm which corresponds to the  $\text{PF}_6^-$  anion. Regarding the  $^{13}\text{C}\{^1\text{H}\}$ -NMR spectra, the most salient feature is that the signal for the  $\text{CS}_2$  moiety is around 91.4–93.3 ppm, which is significantly shielded when compared to complexes **21–27**. This shift to high field is in agreement with the change of hybridization of the  $\text{CS}_2$  carbon atom from  $\text{sp}^2$  to  $\text{sp}^3$  upon incorporation of the methoxy group.

Single crystals of *syn*-**34** suitable X-ray diffraction were obtained from a saturated solution of the compound in THF layered with hexane. The molecular structure displaying the atomic numbering scheme is shown in Fig. 4.

X-Ray diffraction studies revealed a mononuclear compound where the dithio ligand is now  $\kappa^2\text{S,S'}$  coordinated to the gold centre; however, the involved distances S2–Au1 and S3–Au1 are 2.347 Å and 2.285 Å, respectively, with difference being attributed to the higher *trans*-influence of the  $\text{C}_6\text{H}_4$  aromatic ring when compared to that of the S=P moiety.

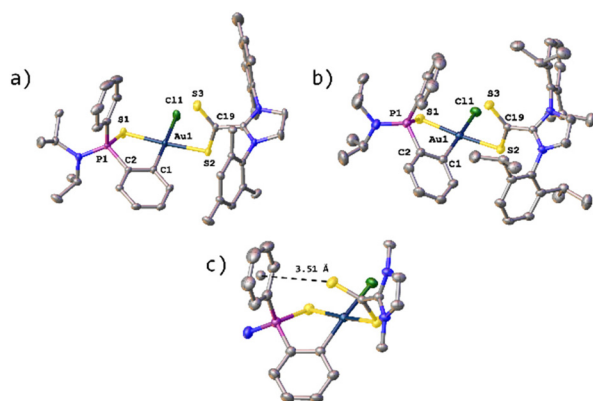
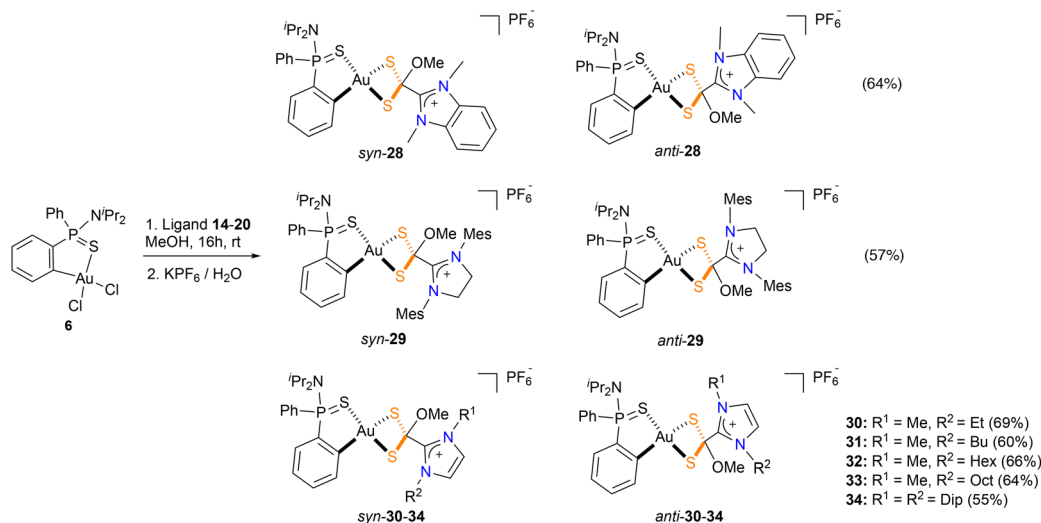


**Fig. 3** Molecular structure of compounds **22** (a) and **27** (b) with hydrogen atoms, solvent molecules and  $\text{PF}_6^-$  anions omitted for clarity. (c) S–Ph  $\pi$  interaction in complex **27**.



**Scheme 3** Synthesis of azol(in)ium-2-(methoxy)methanedithiol complexes **28–34**.

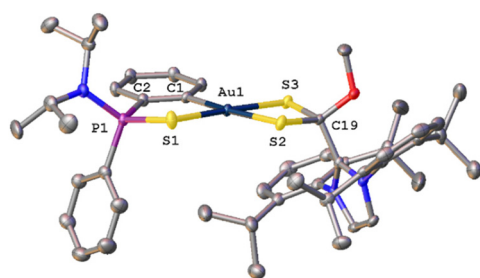
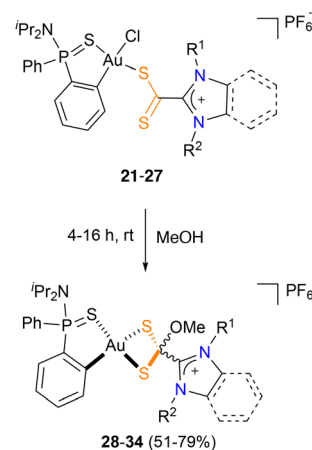


**Fig. 4** Molecular structure of compound *syn*-**34** (H atoms, solvent molecules and  $\text{PF}_6^-$  anion are omitted for clarity).

Furthermore, the distance of the dative  $\text{S1-Au1}$  bond is 2.347 Å, the same as the  $\text{S2-Au1}$  distance. As suggested by the NMR data, the carbon atom of the  $\text{CS}_2$  core has changed hybridization from  $\text{sp}^2$  to  $\text{sp}^3$  during the reaction and has a methoxy group attached. Analogous to complexes **21–27**, the metallacycle deviates slightly from the planar geometry, with the phenylphosphinothioic amide ligand tilted to give a dihedral angle of  $15.03^\circ$ . The value of structural parameter  $\tau_4$  (0.10) suggest that the geometry around the gold atom is pseudo-square planar.<sup>19</sup>

To investigate the possible transformation of dithiocarboxylate into dithiolate complexes, compounds **21–27** were dissolved in methanol. After stirring the resulting mixture for a few minutes, the solution turned from red to yellow, suggesting the transformation of the starting azol(in)ium-2-dithiocarboxylate complexes **21–27** into the azol(in)ium-2-(methoxy)methanedithiolates **28–34**. After 6 h (20 h for sterically hindered complexes **22** and **27**), the corresponding dithiolate complexes **28–34** were isolated in almost quantitative yield (Scheme 4).

In order to gain more insight on this unusual transformation, we monitored this transformation by  $^{31}\text{P}$ -NMR. Thus, an



**Scheme 4** Transformation of azol(in)ium-2-dithiocarboxylate complexes **21–27** into azol(in)ium-2-(methoxy)methanedithiol complexes **28–34**.

NMR tube was charged with **27** and deuterated methanol was added;  $^{31}\text{P}$ -NMR spectra were recorded at ten-minute intervals (Fig. S56 and S57, ESI†). Formation of significant amounts of **34** is evident after just 10 min of reaction and the complete disappearance of the starting dicarboxylate complex **27** takes 4.5 h. Interestingly, a new resonance appears after *ca.* 10 min of reaction in a intermediate position between the resonances of the parent chloride and those of the cyclometallated derivative **34** ( $\delta_{\text{P}} = 69$  ppm), and it completely disappears after *ca.* 5 hours. This new signal must be attributed to the formation of a long-lived reaction intermediate and can be tentatively assigned to a putative  $\text{Au(III)}$  complex derivative formed after metathesis of the chloride ligand by a methoxy (*vide infra*).

Aiming to shed some light into the transformation of 2-dithiocarboxylate complexes **21–27** into (methoxy)methanedithiolate complexes **28–34**, we decided to explore the mecha-



nism for such process by means of DFT calculations. To that end, we have used as model compound the 1,3-bis(2,6-diisopropylphenyl)-1*H*-imidazol-3-ium derivative **27**. According to our calculations, the first step of the reaction would be a Cl to OMe ligand metathesis whereby a new gold methoxide complex (**I1**) is formed after formal HCl elimination (Fig. S58, ESI†). This substitution takes place through a transition state (**TS1**, Fig. 5) of moderate activation energy (*ca.* 10 kcal mol<sup>−1</sup> above the starting chloride *trans*-**27**), and is preceded by the formation of a methanol adduct (*trans*-**27**·MeOH), in which the solvent molecule is bound by a strong MeOH...Cl hydrogen bond ( $d_{\text{H}\cdots\text{Cl}} = 2.38$  Å), an interaction not altering significantly the coordination sphere of the gold atom. The gold centre in **TS1** displays a five-coordinate distorted trigonal bipyramidal geometry which agrees with a classification of the overall process as an associative interchange mechanism (*I<sub>a</sub>*), in which Au–Cl bond has been significantly elongated (*ca.* 0.6 Å) with concerted Au–O bond formation ( $d_{\text{Au}\cdots\text{O}} = 2.34$  Å). Similar mechanisms have been proposed on the basis of computational studies for related chloride ligand substitution reactions at Au(III) complexes.<sup>21</sup>

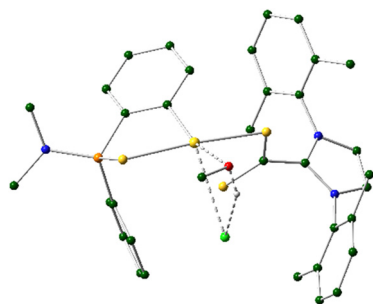


Fig. 5 DFT computed structure of **TS1** with most hydrogen atoms omitted for clarity.

The gold methoxide intermediate **I1** can be, tentatively, identified as the experimentally observed intermediate during the NMR monitoring experiments. Several potential pathways have been explored computationally to account for the transformation of this methoxide **I1** into the final (methoxy)methanedithiolates **34**. According to our calculations, the most likely mechanism would imply the participation of a second molecule of MeOH in the process in an essentially outer-sphere mechanism by which the gold atom is not directly involved in the process (Fig. 6). Thus, in first place the imidazoliumdithiolate group swings so that the sulfur atoms of the CS<sub>2</sub> group exchange its positions to form intermediate **I1'**, a process with a small energy penalty (*ca.* 6 kcal mol<sup>−1</sup>) occurring through an energetically accessible **TS2** located only +11 kcal mol<sup>−1</sup> above **I1**. Then, addition of MeOH occurs in an exergonic manner (*ca.* −2 kcal mol<sup>−1</sup>) rendering the formation of **I1'**·MeOH adduct, in which the incoming solvent molecule binds to the Au bound methoxide group through a conventional strong hydrogen bond interaction ( $d_{\text{O}\cdots\text{H}} = 1.692$  Å), while an almost perfect orientation of the oxygen atom of the methanol molecule to accomplish the nucleophilic attack to the carbon atom of the CS<sub>2</sub> group is attained ( $d_{\text{O}\cdots\text{C}} = 3.031$  Å). NBO analysis of the charges in this intermediate also provides additional support for the nucleophilic attack ( $q_{\text{O}} = -0.682e$ ,  $q_{\text{C}} = +0.445e$ ), which occurs through transition state **TS3** which is located *ca.* 19 kcal mol<sup>−1</sup> above the parent methoxide **I1**. Interestingly, the formation of the new C–O bond in **TS3** ( $d_{\text{CO}} = 2.029$  Å) occurs in a concerted manner with a proton transfer from the former methanol to the gold bound methoxide, with the hydrogen atom being, in fact, more tightly bound to this latter group ( $d_{\text{OH}} = 1.082$  and 1.412 Å, respectively).

The outcome of this step is the formation of a new intermediate (**I2**) placed *ca.* +12 kcal mol<sup>−1</sup> above **I1** and displaying a fully formed (methoxy)methanedithiolate group which is bound to the gold centre in a κ<sup>1</sup>S-monodentate mode, while the former methoxide group also remains coordinated to the

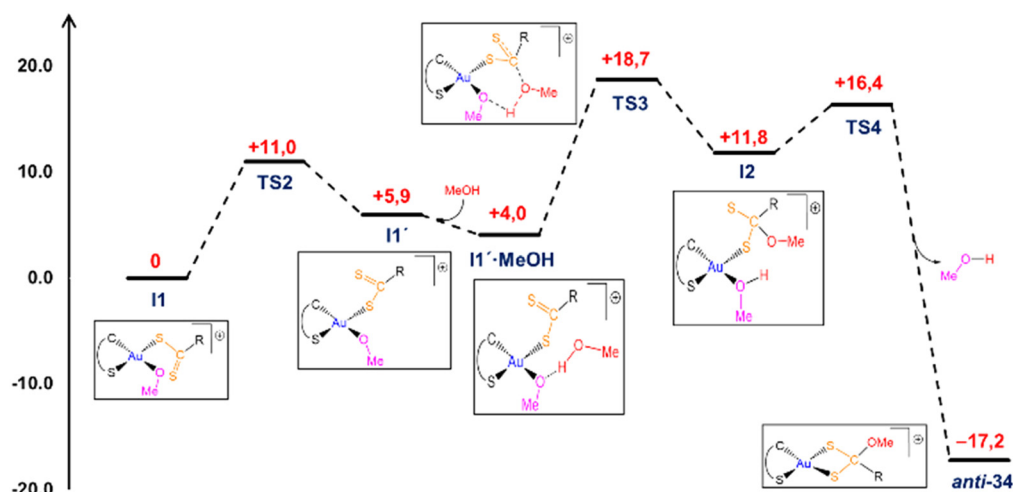


Fig. 6 DFT computed reaction profile for the **I1** → *anti*-**34** transformation.



metal now converted into a methanol molecule. From here, the system would evolve by methanol replacement by the non-coordinated sulfur atom of the dithiolate group, leading to the formation of the reaction product displaying an *anti* configuration (*anti*-**34**). This ligand substitution occurs through an energetically accessible **TS4** (*ca.* +16 kcal mol<sup>-1</sup>), and also follows an associative interchange mechanism, with concerted elimination of methanol ( $d_{\text{AuO}} = 2.434 \text{ \AA}$ ) and formation of Au-S bond ( $d_{\text{AuS}} = 2.896 \text{ \AA}$ ). Considering the complete mechanism, the rate determining step for the **I1** to *anti*-**34** transformation would correspond to the nucleophilic attack of the methanol oxygen atom to the carbon atom of the CS<sub>2</sub> group with an overall reaction barrier of *ca.* 19 kcal mol<sup>-1</sup>, which is kinetically accessible at room temperature. In order to account for the formation of the corresponding *syn*-**34** isomer, a similar mechanism has been computationally verified (Fig. S59, ESI†) with the main differences then being that the initial coordination of the methanol molecule would take place directly at the methoxide **I1** and that the overall energetic barrier would be slightly higher ( $\Delta\Delta G^\ddagger = +1.6 \text{ kcal mol}^{-1}$ ), yet remaining compatible with a room temperature transformation, and accounting for the experimental observation of formation of both *syn*- and *anti*-isomers of **34**.

### Catalytic activity of the synthesized Au(III) complexes

As mentioned before, one of the most relevant applications of Au(III) complexes is as catalysts in the activation of unsaturated bonds. To this end, it is of the uttermost importance to reach the right balance between stability and reactivity. In this regard, we hypothesized that cationic (S<sup>+</sup>C, S<sup>+</sup>S)-cyclometallated gold(III) complexes might be able to stabilize the cationic Au(III) center while maintaining catalytic activity. In order to evaluate the catalytic performance of  $\kappa^1\text{S}$ -azol(in)ium-2-dithiocarboxylate complexes **21–27** and  $\kappa^2\text{S,S}$ -azol(in)ium-2-

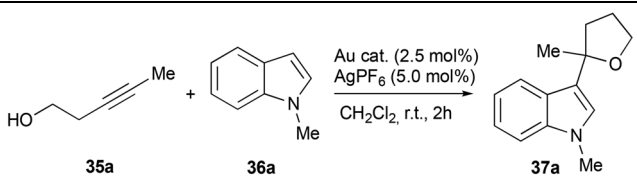
(methoxy)methanedithiolate complexes **28–34**, we focused on the Au(III)-catalyzed preparation of 3-substituted indoles,<sup>22</sup> important structural motifs found in many natural products and pharmaceuticals.<sup>23</sup>

With the aim of investigating the catalytic activities of  $\kappa^1\text{S}$ -azol(in)ium-2-dithiocarboxylate complexes **21–27** and  $\kappa^2\text{S,S}$ -azol(in)ium-2-(methoxy)methanedithiolate complexes **28–34** in the gold–silver cooperative dual catalytic alkylation of indoles, the reaction of alkynyl alcohol **35a** with indole **36a** was used as a model. The results of the catalytic studies are given in Table 1.

Using 2.5 mol% of azol(in)ium-2-dithiocarboxylate complexes **21–27** (2.5 mol%) with AgPF<sub>6</sub> (5 mol%), alkylated indole **37a** was obtained in good yields in all cases (entries 1–7).

In contrast, azol(in)ium-2-(methoxy)methanedithiolate complexes **28–34** displayed very poor catalytic activity (entries 8 and 9). This result is in agreement with the findings obtained by DFT calculations, which show a high stability of the Au(III) centre in the azol(in)ium-2-(methoxy)methanedithiolate complexes. Therefore, the monocyclometallated Au(III) center in the azol(in)ium-2-dithiocarboxylate complexes can effectively activate the alkyne moiety, whereas the cyclometallated Au(III) center in the azol(in)ium-2-(methoxy)methanedithiolate complexes is too stable to undergo any type of reaction. The best results were obtained with complex **22**, affording alkylated indole **37a** in an excellent 97% yield (entry 2). In general terms, the catalytic activity increases with increasing size of the side chain in the azol(in)ium moiety. This trend could be related to differences in the geometry of the complexes, since bulkier ligands somehow distort the square planar geometry of the metal center. In this regard, it has been reported that distorted square planar geometry in Au(III) complexes is associated with enhanced catalytic activity.<sup>22a</sup> In the control experiments (entries 10 and 11), only low yields were observed when a single metal catalyst was used.

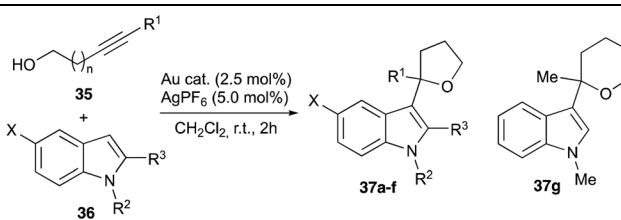
**Table 1** Screening of conditions for the synthesis of alkylated indoles



Entry	Au catalyst (mol%)	Ag catalyst (mol%)	Yield <sup>a</sup> (%)
1	<b>21</b> (2.5)	AgPF <sub>6</sub> (5)	94
2	<b>22</b> (2.5)	AgPF <sub>6</sub> (5)	97
3	<b>23</b> (2.5)	AgPF <sub>6</sub> (5)	78
4	<b>24</b> (2.5)	AgPF <sub>6</sub> (5)	80
5	<b>25</b> (2.5)	AgPF <sub>6</sub> (5)	85
6	<b>26</b> (2.5)	AgPF <sub>6</sub> (5)	88
7	<b>27</b> (2.5)	AgPF <sub>6</sub> (5)	84
8	<b>28</b> (2.5)	AgPF <sub>6</sub> (5)	6
9	<b>29</b> (2.5)	AgPF <sub>6</sub> (5)	8
10	<b>22</b> (2.5)	—	0
11	—	AgPF <sub>6</sub> (5)	6

<sup>a</sup> Determined by <sup>1</sup>H NMR using 1,3,5-trimethoxybenzene as an internal standard.

**Table 2** Gold(III) complex-silver catalyzed cyclization–addition reactions of alkynyl alcohols **35** and substituted indoles **36**



Entry	35	R <sup>1</sup>	n	36	R <sup>2</sup>	R <sup>3</sup>	X	37	Yield <sup>a</sup> (%)
1	<b>a</b>	Me	1	<b>a</b>	Me	H	H	<b>a</b>	97
2	<b>b</b>	Et	1	<b>a</b>	Me	H	H	<b>b</b>	95
3	<b>c</b>	Bu	1	<b>a</b>	Me	H	H	<b>c</b>	91
4	<b>a</b>	Me	1	<b>b</b>	Me	H	Br	<b>d</b>	95
5	<b>b</b>	Et	1	<b>b</b>	Me	H	Br	<b>e</b>	98
6	<b>a</b>	Me	1	<b>c</b>	H	Me	H	<b>f</b>	71
7	<b>d</b>	Me	2	<b>a</b>	Me	H	H	<b>g</b>	89

<sup>a</sup> Determined by <sup>1</sup>H NMR using 1,3,5-trimethoxybenzene as an internal standard.



Using the optimized conditions, we investigated the substrate scope of the dual metal catalysis for indole alkylation. Thus, a solution of alkynyl alcohol **35** and indole **36** in  $\text{CH}_2\text{Cl}_2$  in the presence of a 2.5 mol% of complex **22** and a 5 mol% of  $\text{AgPF}_6$  was stirred at r.t. for 2 h.

According to the results compiled on Table 2, alkynyl alcohols of different chain lengths **35a–d** and indoles with different substituents **36a–b** afforded alkylated indoles **37a–e** with good to excellent yields (71–97%) and total regioselectivity. The reactivity and regioselectivity observed for the indole alkylation reaction were consistent with those reported in the literature.<sup>22a,24</sup>

## Conclusions

In conclusion, we have described the preparation and characterization of a novel family of Au(III) cyclometallated  $\kappa^1\text{S}$ -azol(in)ium-2-dithiocarboxylate complexes. These derivatives undergo a fascinating rearrangement in the presence of methanol to afford the corresponding Au(III) cyclometallated  $\kappa^2\text{-S,S'}$ -azol(in)ium-2-(methoxy)methanedithiolate complexes, a family of Au(III) compounds that have no precedent in the literature. In addition, this transformation was thoroughly investigated by the means of NMR studies and DFT calculations, allowing us to propose a plausible mechanism.

Furthermore, the catalytic behavior of both families of Au(III) complexes in the alkylation of indoles has been explored. In this regard,  $\kappa^1\text{S}$ -azol(in)ium-2-dithiocarboxylate complexes display excellent performance, providing alkylated indoles in good to excellent yields and total regioselectivity. On contrary,  $\kappa^2\text{-S,S'}$ -azol(in)ium-2-(methoxy)methanedithiolate complexes showed poor catalytic activity, consistent with their high stability, as predicted by the DFT calculations.

## Author contributions

Conceptualization: R. G. S., H. R. S.; investigation: P. P. R., M. A. M., R. G. S., D. E., D. G. V.; validation: P. P. R., R. G. S.; supervision: R. G. S., H. R. S., D. E.; funding acquisition: R. G. S., H. R. S.; project administration: R. G. S., H. R. S.; writing – original draft: R. G. S., D. E.; writing – review & editing: R. G. S., H. R. S., D. E., D. G. V., P. P. R., M. A. M.

## Conflicts of interest

All authors declare that they have no conflicts of interest.

## Acknowledgements

This work has received financial support from the Instituto de Salud Carlos III (PI22/00148) and MINECO (PID2022-137893OB-I00 and PID2021-123964NB-I00). Partial financial support by Instituto de Salud Global de Barcelona (FUO-23-

194) is gratefully acknowledged. We thank the SCBI of the Universidad de Málaga, Spain, for access to computing facilities. Authors would like to thank the use of RIAIDT-USC analytical facilities. P. P. R. thanks Programa Investigo for a predoctoral contract (AYUD/2022/9313, EU Next Generation).

## References

- (a) D. J. Gorin and F. D. Toste, *Nature*, 2007, **446**, 395; (b) Z. Li, C. Brouwer and C. He, *Chem. Rev.*, 2008, **108**, 3239; (c) A. Corma, A. Leyva-Pérez and M. J. Sabater, *Chem. Rev.*, 2011, **111**, 1657; (d) J. Ruiz, D. Sol, M. A. Mateo, M. Vivanco and R. Badía-Laiño, *Dalton Trans.*, 2020, **49**, 6561; (e) G. Moreno-Alcántar, P. Picchetti and A. Casini, *Angew. Chem., Int. Ed.*, 2023, **62**, 1433; (f) P. Crochet and V. Cadierno, *Catalysts*, 2023, **13**, 436.
- (a) B. D. Glišić and M. I. Djuran, *Dalton Trans.*, 2014, **43**, 5950; (b) D. Fontinha, S. A. Sousa, T. S. Morais, M. Prudencio, J. H. Leitao, Y. Le Gal, D. Lorcy, R. A. L. Silva, M. F. G. Velho, D. Belo, M. Almeida, J. F. Guerreiro, T. Pinheiro and F. Marques, *Metallomics*, 2020, **12**, 974.
- (a) V. W.-W. Yam and A. S.-Y. Law, *Coord. Chem. Rev.*, 2020, **414**, 213298; (b) V. W.-W. Yam, K. M.-C. Wong, L.-L. Hung and N. Zhu, *Angew. Chem.*, 2005, **117**, 3167.
- (a) A. Arcadi and S. Di Giuseppe, *Curr. Org. Chem.*, 2004, **8**, 795; (b) H. Schmidbaur and A. Schier, *Arabian J. Sci. Eng.*, 2012, **37**, 1187.
- (a) L. Rocchigiani and M. Bochmann, *Chem. Rev.*, 2021, **121**, 8364; (b) M. N. Hopkinson, A. D. Gee and V. Gouverneur, *Chem. – Eur. J.*, 2011, **17**, 8248; (c) T. C. Boorman and I. Larrosa, *Chem. Soc. Rev.*, 2011, **40**, 1910; (d) P. Garcia, M. Malacria, C. Aubert, V. Gandon and L. Fensterbank, *ChemCatChem*, 2010, **2**, 493; (e) H. A. Wegner and M. Auzias, *Angew. Chem., Int. Ed.*, 2011, **50**, 8236.
- E. A. Pacheco, E. R. T. Tiekink and M. W. Whitehouse, *Gold Chemistry*, Wiley-VCH Verlag GmbH & Co. KGaA, 2009, vol. 283.
- (a) B. Bertrand and A. Casini, *Dalton Trans.*, 2014, **43**, 4209; (b) E. Belmonte-Sánchez, M. J. Iglesias, H. El Hajjoui, L. Rocas, S. García-Granda, P. Villuendas and F. López-Ortiz, *Organometallics*, 2017, **36**, 1962.
- (a) I. Özdemir, N. Tenelli, S. Günel and S. Demir, *Molecules*, 2010, **15**, 2203; (b) S. Hussaini, R. A. Haque and M. R. Razali, *J. Organomet. Chem.*, 2019, **882**, 96.
- (a) L. Delaude, A. Demonceau and J. Wouters, *Eur. J. Inorg. Chem.*, 2009, 1882; (b) O. Sereda, A. Blanrue and R. Wilhelm, *Chem. Commun.*, 2009, 1040; (c) D. Konieczna, A. Blanrue and R. Wilhelm, *Z. Naturforsch., B: Anorg. Chem., Org. Chem.*, 2014, **69**, 596; (d) P. A. Gokturk, S. E. Donmez, B. Ulgut, Y. E. Türkmen and S. Suzer, *New J. Chem.*, 2017, **41**, 10299; (e) L. Di Marco, M. Hans, L. Delaude and J.-C. M. Monbaliu, *Chem. – Eur. J.*, 2016, **22**, 4508; (f) F. Mazars, M. Hrubaru, N. Tumanov, J. Wouters and L. Delaude, *Eur. J. Org. Chem.*, 2021, 2025;



- (g) A. R. Katritzky, D. Jishkariani, R. Sakhuja, C. D. Hall and P. J. Steel, *J. Org. Chem.*, 2011, **76**, 4082.
- 10 (a) T. F. Beltrán, G. Zaragoza and L. Delaude, *Dalton Trans.*, 2017, **46**, 9036; (b) T. F. Beltrán and L. Delaude, *J. Cluster Sci.*, 2017, **28**, 667; (c) D. Elorriaga, B. Parra-Cadenas, P. Pérez-Ramos, R. G. Soengas, F. Carrillo-Hermosilla and H. Rodríguez-Solla, *Crystals*, 2023, **13**, 1304.
- 11 L. L. Borer, J. V. Kong, P. A. Keihl and D. M. Forkey, *Inorg. Chim. Acta*, 1987, **129**, 223.
- 12 S. Naeem, L. Delaude, A. J. P. White and J. D. E. T. Wilton-Ely, *Inorg. Chem.*, 2010, **49**, 1784.
- 13 U. Siemeling, H. Memczak, C. Bruhn, F. Vogel, F. Träger, J. E. Baio and T. Weidner, *Dalton Trans.*, 2012, **41**, 2986.
- 14 (a) C. Ratia, V. Cepas, R. Soengas, Y. Navarro, M. Velasco-de Andrés, M. J. Iglesias, F. Lozano, F. López-Ortiz and S. M. Soto, *Front. Microbiol.*, 2022, **13**, 815622; (b) C. Ratia, S. Sueiro, R. G. Soengas, M. J. Iglesias, F. López-Ortiz and S. M. Soto, *Antibiotics*, 2022, **11**, 1728; (c) C. Ratia, V. Ballén, Y. Gabasa, R. Soengas, I. A. Velasco-de, M. J. Iglesias, Q. Cheng, F. Lozano, E. S. J. Arnér, F. López-Ortiz and S. M. Soto, *Front. Microbiol.*, 2023, **14**, 1198473.
- 15 R. Navarro and E. P. Urriolabeitia, *J. Chem. Soc., Dalton Trans.*, 1999, 4111.
- 16 R. G. Pearson, *Inorg. Chem.*, 1973, **12**, 712.
- 17 (a) A. L. Thompson, L. Delaude and J. D. E. T. Wilton-Ely, *Chem. – Eur. J.*, 2010, **16**, 1097; (b) T. F. Beltrán, G. Zaragoza and L. Delaude, *Polyhedron*, 2021, **197**, 115055; (c) M. Z. Aldin, G. Zaragoza, W. Deschamps, J.-C. D. Tomani, J. Souopgui and L. Delaude, *Inorg. Chem.*, 2021, **60**, 16769.
- 18 F. H. Allen, D. G. Watson, L. Brammer, A. G. Orpen and R. Taylor, in *International Tables for Crystallography*, ed. E. Prince, Springer, Berlin, 2006, vol. C, pp. 790–811.
- 19 J. Hwang, P. Li, M. D. Smith, C. E. Warden, D. A. Sirianni, E. C. Vik, J. M. Maier, C. J. Yehl, C. D. Sherrill and K. D. Shimizu, *J. Am. Chem. Soc.*, 2018, **140**, 13301.
- 20 L. Yang, D. R. Powell and R. P. Houser, *Dalton Trans.*, 2007, 955.
- 21 (a) A. Djeković, B. Petrović, Ž. D. Bugarčić, R. Puchtab and R. van Eldik, *Dalton Trans.*, 2012, **41**, 3633; (b) H. F. Dos Santos, D. Paschoal and J. V. Burda, *Chem. Phys. Lett.*, 2012, **548**, 64.
- 22 (a) H.-M. Ko, K. K.-Y. Kung, J.-F. Cui and M.-K. Wong, *Chem. Commun.*, 2013, **49**, 8869; (b) J. Rodríguez, A. Zeineddine, E. D. Sosa Carrizo, K. Miqueu, N. Saffon-Merceron, A. Amgouné and D. Bourissou, *Chem. Sci.*, 2019, **10**, 7183.
- 23 (a) N. Chadha and O. Silakari, *Eur. J. Med. Chem.*, 2017, **134**, 159; (b) A. Dorababu, *RSC Med. Chem.*, 2020, **11**, 1335; (c) D. Sarkar, A. Amin, T. Qadir and P. K. Sharma, *Open Med. Chem. J.*, 2021, **15**, 1; (d) N. G. Bajad, S. K. Singh, S. K. T. D. Singh and M. Singh, *Curr. Res. Pharmacol. Drug Discov.*, 2022, **3**, 100119; (e) P. A. Pacheco and M. M. Santos, *Molecules*, 2022, **27**, 319.
- 24 S. Bhuvaneswari, M. Jeganmohan and C.-H. Cheng, *Chem. – Eur. J.*, 2007, **13**, 8285.

